Journal of Physics: Conference Series **160** (2009) 012027 doi:10.1088/1742-6596/160/1/012027

Calibration and Monitoring of a Scintillator HCAL with SiPMs CALICE Scintillator HCAL

Angela Lucaci-Timoce (on behalf of the CALICE collaboration)
DESY, Notkestr. 85, 22607 Hamburg, Germany

E-mail: angela-isabela.lucaci-timoce@desy.de

Abstract. The operational experience with a highly-granular analogue hadronic calorimeter (AHCAL) consisting of 7608 individual scintillator tiles readout via Silicon-Photo-multipliers (SiPM) is presented. The calibration of each cell is based on minimum ionizing particle signals for which in general a muon beam is used. In addition, a correction for the non-linearity introduced by the finite number of pixels (1156) in the SiPM is applied. The aspects of temperature and voltage dependence of SiPM are addressed, and monitoring and calibration procedures are discussed. Such procedures are essential for the extrapolation of calibration factors over several days of data taking with the calorimeter. For this purpose a versatile UV-LED light distribution system was developed, capable of delivering light to all tiles with intensity from a few photo-electrons to the saturation of the SiPM. The procedures are tested using data collected with the AHCAL at the CERN SPS test beam.

1. Introduction

The CALICE collaboration built a high granularity calorimeter prototype for a future high energy electron positron linear collider. In view of testing shower simulation and validating the particle flow approach, data were taken in the years 2006 and 2007 at CERN SPS test beam. For a discussion of the physics results, see [1]. The technical solutions for a realistic calorimeter, like mechanical design and DAQ, are presented in [2].

The response of SiPMs depends on temperature and voltage variations. These dependencies are monitored with an LED system, with twelve LEDs per HCAL module. Each LED illuminates 18 SiPMs and one PIN photodiode to monitor the LED signal. The LED system is used to obtain the individual SiPM gain in runs with low LED light intensity (see section 2.3). Another feature of the system is to supply reference pulses monitored by PIN diodes. In addition, it provides the full dynamic range for checking the SiPM response function.

The temperature variations are monitored by five temperature sensors aligned vertically in the center of each AHCAL module.

In case of long data taking periods of several days, the calibration factors extracted in the beginning may be extrapolated at the end of the data taking, with the help of the monitoring system.

2. AHCAL Calibration Chain

The analog signal of the SiPMs is given by the total number of fired pixels. But due to the limited number of pixels (1156) and the finite pixel recovery time (20-500 ns), the SiPMs get

saturated when the numbers of produced photoelectrons is of the order of the total number of pixels. As a result, a non-linear SiPM response curve is obtained (see Figure 1).

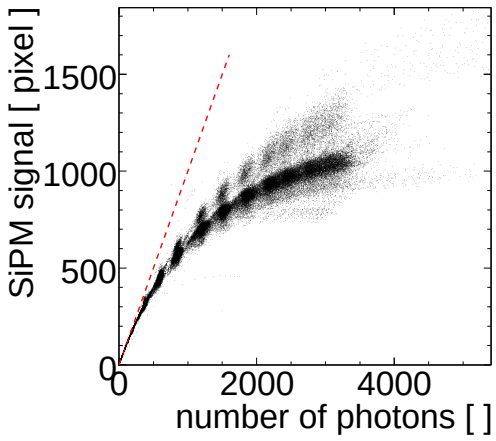

Figure 1. Dependence of the SiPMs signal (in pixels) on the number of produced photoelectrons, measured at ITEP (Russia). The dashed line indicates the linear behaviour. The measurements were done with 'bare' SiPMs (i.e. before being installed on the scintillator tiles) on the test bench.

Each calorimeter cell is calibrated based on signals from minimum ionising particles (MIPs), for which muons are used in a first approximation. The calibration of one cell i is done according to:

$$E_i[MIP] = \frac{A_i[ADC]}{A_i^{MIP}[ADC]} \cdot f_{resp}(A_i[pixels]) \tag{1}$$

where $A_i[ADC]$ is the amplitude registered in cell i, in units of ADC channels, and $A_i^{MIP}[ADC]$ is the MIP amplitude in cell i (see section 2.1). The SiPM response function $f_{resp}(A_i[pixels])$ corrects for the non-linearity of the SiPM response. It acts on the amplitude expressed in number of pixels, and returns the saturation correction factor which needs to be applied to linearize the amplitude in MIPs.

The amplitude in pixels is obtained by dividing the amplitude of a cell by the corresponding SiPM gain $G_i[ADC]$:

$$A_i[pixels] = \frac{A_i[ADC]}{G_i[ADC]}. \tag{2}$$

The procedure to obtain the individual SiPM gain is discussed in section 2.3.

2.1. AHCAL MIP Calibration with Muons

As already mentioned, muons are used as minimum ionising particles in a first approximation. The amplitude spectra of the 216 tiles of each HCAL modules in muon events are fitted with a convolution of Gaussian and Landau distribution (see Figure 2). For reference, the noise distribution obtained with random trigger events is overlayed. The MIP calibration factor is defined as the difference between the most probable value of the minimum ionising peak and the mean of the noise peak.

To reject noise, a cut of 0.5 MIPs is applied. As a result, the MIP uncertainties affect the reconstructed energy and the noise level.

The MIP signal to noise ratio is defined as the ratio between the MIP value and the σ of the noise distribution, and it is a measure of the separation power between the noise and the minimum ionising peak. The distribution of the signal to noise ratio for the data taken in 2006

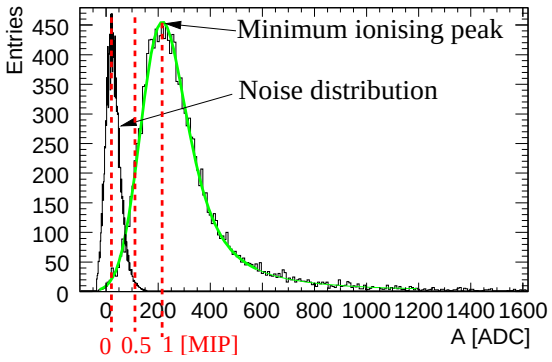

Figure 2. Example of amplitude spectra for an HCAL tile in muon events.

and 2007 is shown in Figure 3. On average, a signal to noise ratio of 9-10, and of 12, was obtained for the year 2007, and 2006, respectively.

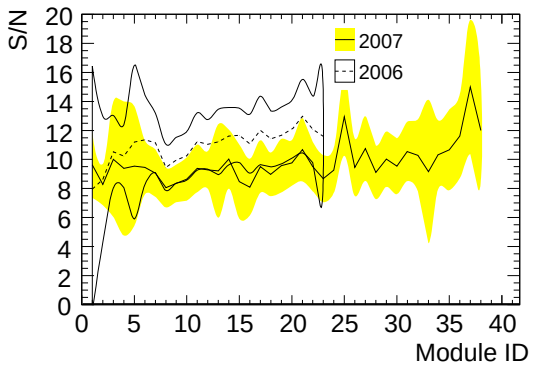

Figure 3. Distribution of the average MIP signal to noise ratio in each AHCAL module for the 2006 and 2007 data taking periods. The error band indicates the spread (RMS) between all cells in one module [3].

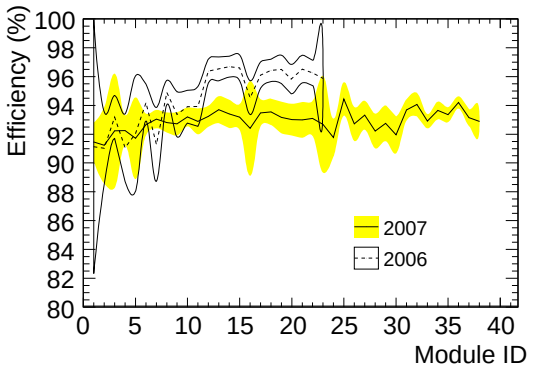

Figure 4. Distribution of the average MIP detection efficiency in each AHCAL module for the 2006 and 2007 data taking periods. The error band indicates the spread (RMS) between all cells in one module [3].

The MIP detection efficiency, defined as the ratio between the MIP value and the σ of the MIP distribution, is presented in Figure 4, for a threshold cut of 0.5 MIPs. An average of 93% and of 96% was obtained in 2007, and 2006, respectively. The difference is due to a decrease of the light yield in the year 2007, due to operation at higher temperatures.

2.2. MIP Calibration with Hadrons

In case of a deep-site detector, which is a possibility for the ILC, cosmic muons may not be enough to calibrate the calorimeter. Therefore, solutions have been looked for of using other types of particles as MIPs instead of muons. One idea, proposed in 2004 by A. Raspereza, was to use hadrons as MIPs. Since their interaction length is high ($\lambda_i \sim 17$ cm, which corresponds to about 8 HCAL layers), long tracks within hadron showers are abundant, and they are good MIP candidates.

The idea was followed by the CALICE group in Munich. Track-like clusters in hadron events were selected based on the deep analysis algorithm of V. Morgunov [7]. The amplitude spectra

of single tiles were fitted with an exponential convoluted with a Landau distribution. For tiles close to the beam axis, a clear MIP peak was observed (see Figure 5), whereas for tiles outside the beam axis, the background is predominant (see Figure 6).

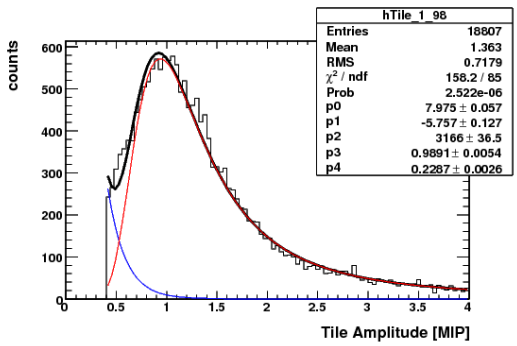

Figure 5. Amplitude spectra for an AHCAL tile close to the beam axis, in hadron events [6].

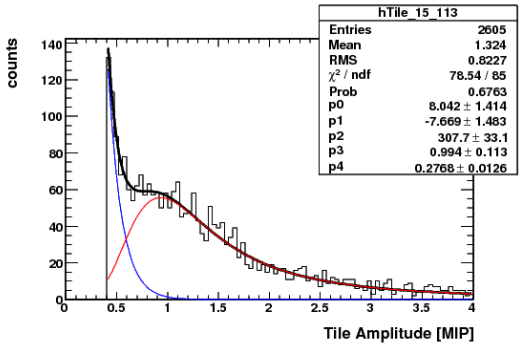

Figure 6. Amplitude spectra for an AHCAL tile outside the beam axis, in hadron events [6].

2.3. Gain Calibration

Since the saturation behaviour of the SiPMs appears at the pixel scale, one needs a way to obtain this scale. This is done via gain calibration, which in addition offers the possibility of looking directly at the SiPMs and monitoring their performance.

The gain calibration is done with the LED system. For all HCAL channels, single photon spectra are taken at low intensity LED light, and fitted with a multi-Gaussian function. An example of such a spectra is shown in Figure 7. The gain value is obtained as the difference between the means of two consecutive single photon peaks. The efficiency of such a calibration is high. For example, for the CERN test-beam data, 96.9% of the channels were calibrated. The rest of 1.7% had the LEDs off, and 1.4% had missing calibration, but these channels were recalibrated at the end of the data taking period, once the detector was back at DESY.

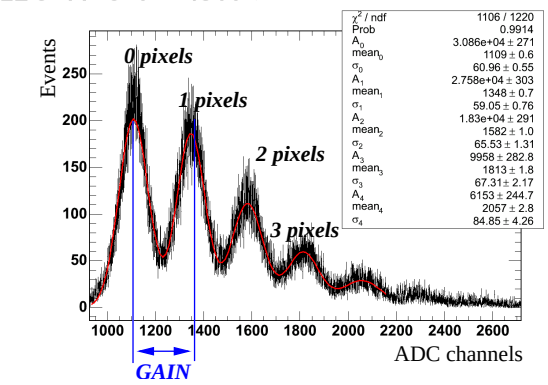

Figure 7. Example of a single photon spectra for an AHCAL channel.

2.4. Saturation Correction

The response function of a SiPM can be approximated by the function:

$$N_{pixel} = N_{total} \cdot \left[1 - \exp\left(-\frac{N_{photoelectrons}}{N_{total}}\right)\right], \tag{3}$$

where N_{total} is the number of pixels at which the SiPMs saturate.

By comparing measurements performed on the 'bare' SiPMs (ITEP) and on the SiPMs mounted on a tile (CERN), the CALICE Bergen group showed that the mounted SiPMs saturate at lower values that 'bare' ones (see Figure 8). This result was later confirmed by the DESY group and by ITEP measurements. The reason is due to geometrical misalignment. The mounted SiPMs do not get completely illuminated by the light cone from the wave length shifting fiber, such that less effective pixels contribute to light detection. To correct for this, a scaling factor $N_{tot}(CERN)/N_{tot}(ITEP)$ was introduced ([5]).

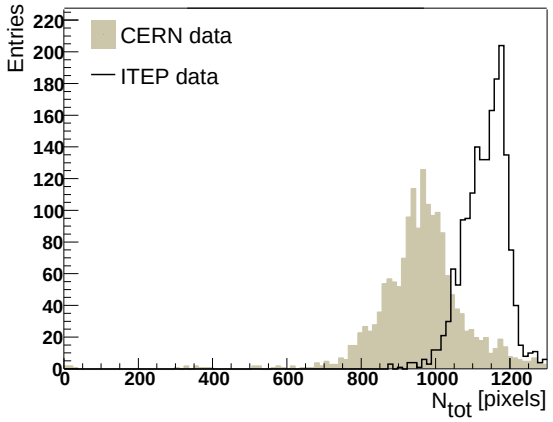

Figure 8. Distribution of the SiPM saturation values: comparison between 'bare' SiPMs (ITEP measurement) and mounted SiPMs (CERN measurement) [4].

3. Time Dependence of the SiPM Response

The SiPMs are operated in Geiger mode, in which the bias voltage is higher than the breakdown voltage:

$$U_{bias} = U_{breakdown}(T) + \Delta U. \tag{4}$$

Typical values for the U_{bias} are 40-70 volts.

The parameters of the SiPMs depend primarly on the overvoltage $\Delta U = U_{bias} - U_{breakdown}(T)$, and indirectly on temperature, via the breakdown voltage.

The SiPM temperature and voltage dependencies can be expressed as:

$$\begin{aligned} G &= G(T,\, U) \\ \epsilon &= \epsilon(T,\, U) \end{aligned} \tag{5}$$

where G is the SiPM intrinsic gain, and ϵ is its photo-detection efficiency.

3.1. SiPM Dependencies on Voltage

The gain and amplitude dependencies on voltage were measured at ITEP, during SiPM production. Depending on the operation point, two groups of SiPMs were observed: group A, operated at about 3 V above breakdown, and group B, operated at about 2 V above breakdown (see Figure 9). The dependencies were well reproduced at the CERN test beam, although a different test set-up was used (see Figures 10 and 11).

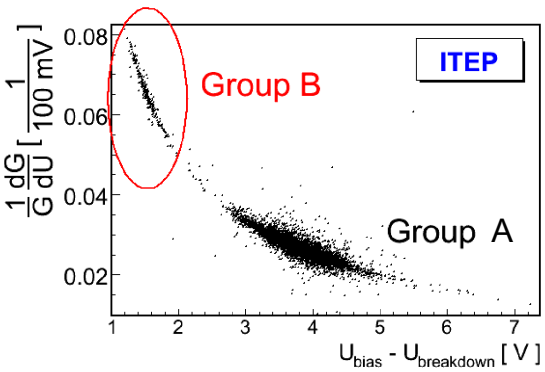

Figure 9. Dependence of the relative SiPM gain on the overvoltage $\Delta U = U_{bias} - U_{breakdown}$ (ITEP measurement).

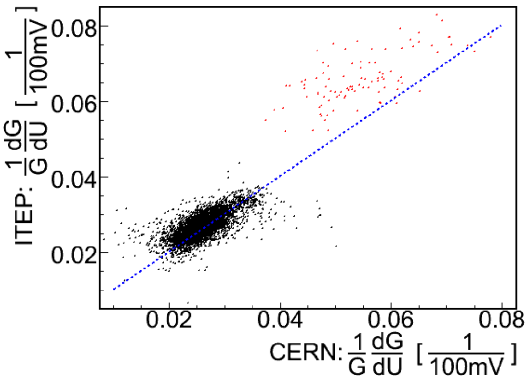

Figure 10. Relative dependencies of **gain** on voltage: comparison between ITEP and CERN measurements. The black points correspond to group A of SiPMs and red to group B (see text for details).

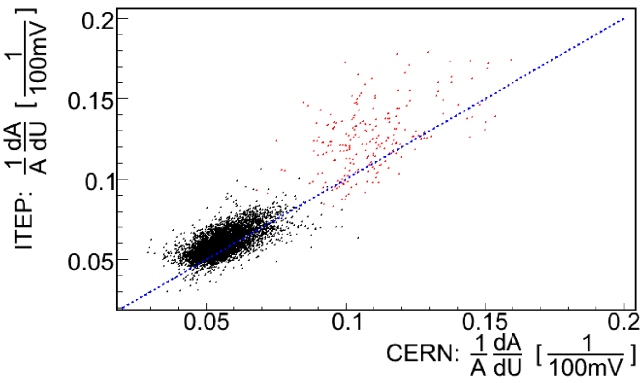

Figure 11. Relative dependencies of **amplitude** on voltage: comparison between ITEP and CERN measurements. The black points correspond to group A of SiPMs and red to group B (see text for details).

3.2. SiPM Response on Temperature Dependence

The temperature variations are measured in test-beam only (i.e. CERN). During one month of data taking, temperature variations of 3-4 degrees are measured. Since the gain depends inversely linear with temperature (see Figure 12), this translates into a variation of $-1.7\% \cdot K^{-1}$ for the gain of the SiPMs from group A. A larger variation, of $-4.0\% \cdot K^{-1}$ for group A, is measured in case of the SiPM amplitude. This is due to the fact that the amplitude is the product of SiPM gain and photo-detection efficiency, both sensitive to temperature variations.

3.3. Voltage Adjustment

The temperature effects on the SiPM gain can be compensated for via voltage adjustement. In a first step, the gain dependence of voltage is fitted with a straight line, and the slope dG/dU is determined. Next, the bias voltage is adjusted to correct for gain deviations:

$$\Delta U = \frac{G - G_0}{dG/dU}, \tag{6}$$

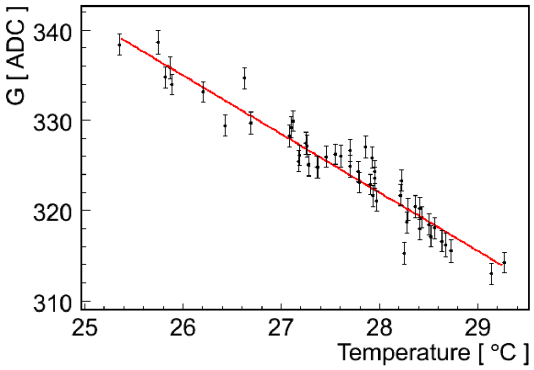

Figure 12. The SiPM gain dependence on temperature.

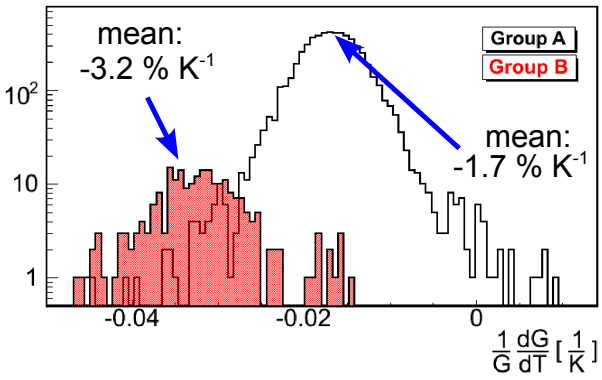

Figure 13. Distribution of the relative gain dependence on temperature.

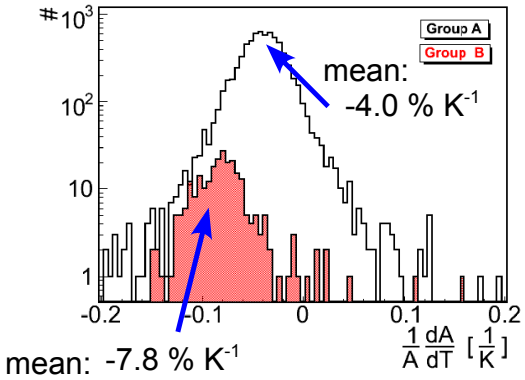

Figure 14. Relative dependence of amplitude on temperature.

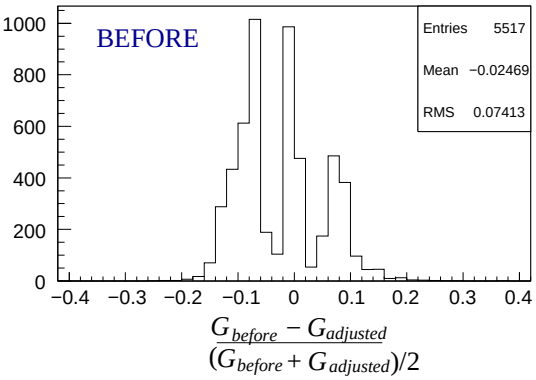

Figure 15. Deviation of the gain from the mean gain, before voltage adjustment.

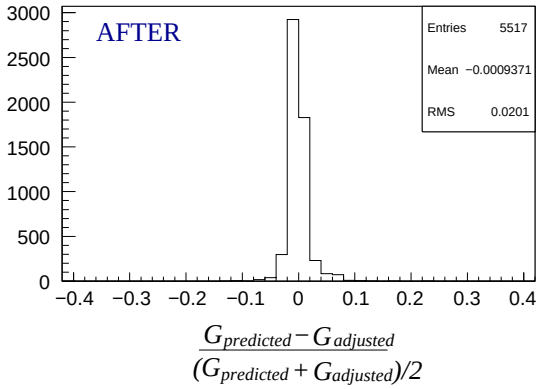

Figure 16. Deviation of the gain from the mean gain, after voltage adjustment.

and the gain $G_{adjusted}$ is measured. The method is checked by comparing the theoretically calculated gain:

$$G_{predicted} = G_{before} + \Delta U \cdot \frac{dG}{dU}, \tag{7}$$

where G_{before} is the gain measured before voltage adjustments, with $G_{adjusted}$.

Figures 15 and 16 show the deviations of the gains difference from the mean, before and after

voltage adjustment. It can be seen that the corrected gain has the expected behaviour.

3.4. Conclusions

The CALICE analog scintillator HCAL is the first experiment to handle large samples of SiPMs (7608 channels in total). The signal of an HCAL cell is calibrated using minimum ionising particles and corrected for the non-linearity of the SiPM response curves. The SiPM performance can be monitored directly via gain calibration. The dependence of the SiPM signal on temperature variations can be corrected for, although the benefits for the data analysis are still to be demonstrated.

3.5. Acknowledgments

This work is supported by Deutsches Elektronen Synchrotron Hamburg.

[1] E. Garutti, these proceedings
[2] F. Sefkow, these proceedings
[3] CALICE collaboration, "The reconstruction of the energy lost by a 120 GeV muon in the highly granular hadronic calorimeter for the International Linear Collider", CALICE note, *CAN-009*
[4] CALICE Bergen group, private communication
[5] CALICE collaboration, "The scintillator ECAL beam test at DESY, 2007", CALICE note, *CAN-012*
[6] F. Simon, "Temperature correction for hadron runs", talk given at the CALICE collaboration meeting in Argonne, USA, 17-19 March, 2008
[7] V. Morgunov and A. Zhelezov, "Deep analysis of hadronic showers", talk given at ILC Software and Tools Workshop, Orsay, 2-4 May, 2007